# Consolidation and Self-Bonding in Poly(ether ether ketone) (PEEK)

**BUM-RAE CHO* and JOHN L. KARDOS**

Materials Research Laboratory, Department of Chemical Engineering, Washington University, St. Louis, Missouri 63130

**SYNOPSIS**

The effects of processing variables (time, temperature, and pressure) on the strength development during self-bonding of amorphous PEEK films were studied using a modified single lap-shear test. It was shown that the self-bonding strength developed isothermally at different bonding temperatures exhibits a linear response with the bonding time raised to the $\frac{1}{4}$ power in agreement with Wool's theory. DSC measurement of the crystallinity produced at different bonding conditions demonstrated that even though PEEK specimens contain the same amount of crystallinity, the resultant self-bonding strength is sensitively dependent on bonding history. C-mode scanning acoustic microscopy (C-SAM) was applied to define the effect of the processing variables on wetting of the bonding area during the bonding process. It was shown that, above a threshold pressure (< 17 psi), the degree of wetting depends weakly on time, but not on temperature. SEM analysis revealed that amorphous PEEK films are self-bonded by crystalline growth after diffusion and entanglement of the polymer chains across the interface. The crystalline growth rate across the interface is much higher at higher temperatures, leading to a higher self-bonding strength. The shear fracture surface observations also support the above result. The PEEK specimens showing the higher self-bonding strengths exhibit much denser striations and deeper dimplelike ductile patterns in the fracture surface, arising from much more crystalline growth across the interface. © 1995 John Wiley & Sons, Inc.

## INTRODUCTION

In recent years, the advent of advanced high-temperature thermoplastic materials has led to their use as substitutes for thermosetting matrix materials in carbon fiber-reinforced composite systems. Among these materials, poly(ether ether ketone) (PEEK), which has a high melting point ($T_m$ = 335°C) and glass transition temperature ($T_g$ = 143°C), has shown significant potential for expanding the spectrum of aerospace applications. The characteristics of PEEK as a new advanced structural material and its application in aerospace structures have been numerously reported.[1-6]

Some practical problems have arisen, however, which require a more careful assessment of the basic physics of these materials. First, in recent years, one of the major concerns of the aerospace composites industry has been the resistance to delamination growth under static or cyclic loading. Apparently, well-consolidated thermoplastic laminates produced under manufacturers' recommended processing cycles have exhibited particularly poor compression strength for drilled-hole laminates. Examinations have revealed that failure initiated at the hole via a ply delamination mechanism. Therefore, to reduce this delamination phenomenon, the development of better bonding between plies of these materials is a critical step in the aerospace manufacturing process. Second, the resultant bond strength of advanced high-temperature thermoplastic resins and composites seems to be highly sensitive to processing variables in the mold.[7,8] Examining the effect of these processing variables on interface consolidation is valuable in evaluating the optimum processing conditions for self-bonding between the glass transition temperature and the melting point. Third, self-bonding at a temperature above the material's

* To whom correspondence should be addressed.

Journal of Applied Polymer Science, Vol. 56, 1435–1454 (1995)
 CCC 0021-8995/95/111435-20

glass transition temperature and below its melting region occurs as a function of time without any adhesives.[9–14] The resultant bond strength approaches that of the virgin state. All three of these phenomena may well be linked to the surface molecular mobility at the polymer–polymer interface.

In this study, a systematic examination of the surface physics and the bonding mechanics for the amorphous PEEK material was accomplished to determine the optimum processing conditions for self-bonding of PEEK and to improve the bond strength between plies of a laminate of this material.

## EXPERIMENTAL

### Material

The material used in this research was Stabar K200, an amorphous thermoplastic PEEK film with a thickness of 20 mil supplied by Imperial Chemical Industry (ICI) Americas Inc.

### Bonding Conditions

Figure 1 shows a typical DSC scan of amorphous PEEK films. To examine the bonding behavior of PEEK as a function of the crystallization temperature, the whole temperature range of the DSC scan of PEEK was divided into three distinct regions as follows:

Region I: above the glass transition (143°C) and below the cold crystallization region (165°C).
Region II: cold crystallization region (165–185°C).
Region III: above the cold crystallization (185°C) and below the melting region.

From these regions, seven different bonding temperatures were selected as follows:

150°C and 160°C from Region I.
175°C from Region II.
200°C, 250°C, 270°C, and 300°C from Region III.

At each temperature, PEEK specimens were bonded for three different times: 1, 3.5, and 10 h.

### Bonding Procedure

As-received amorphous PEEK film was cut and sized for making a modified single lap-shear joint speci-

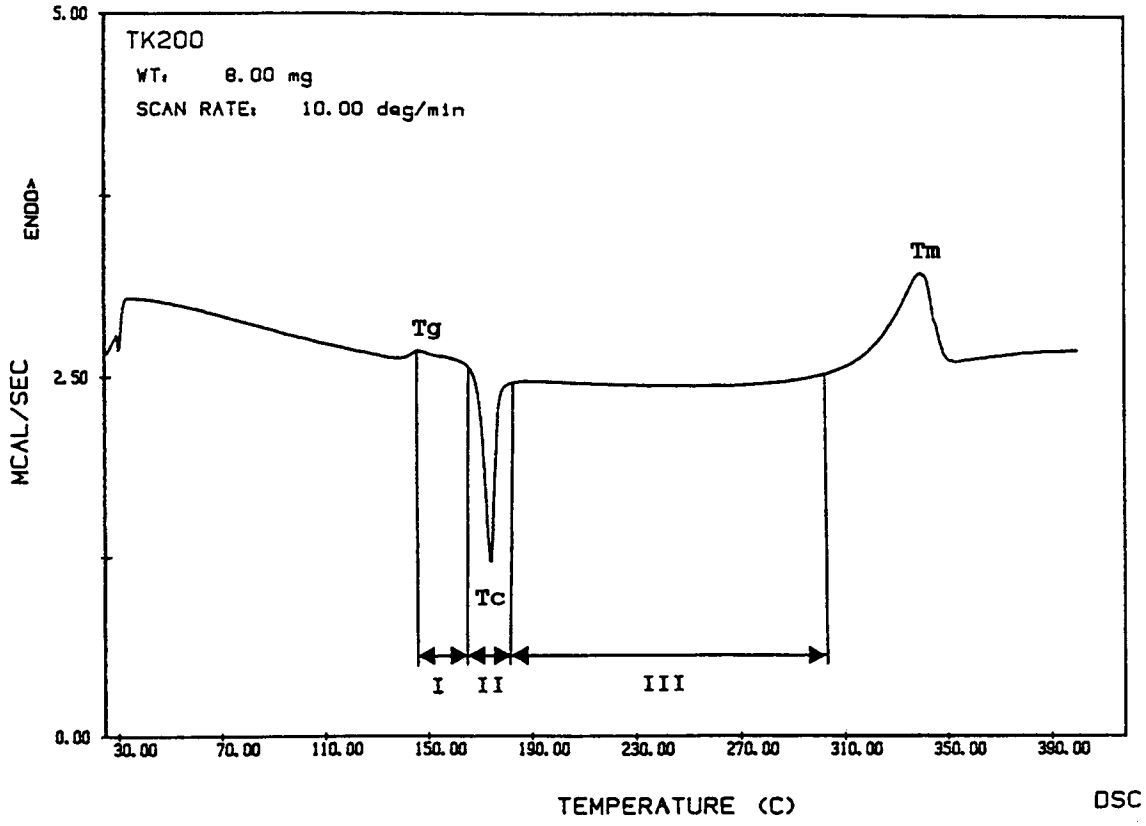


**Figure 1** Three distinct temperature regions for the self-bonding of PEEK.

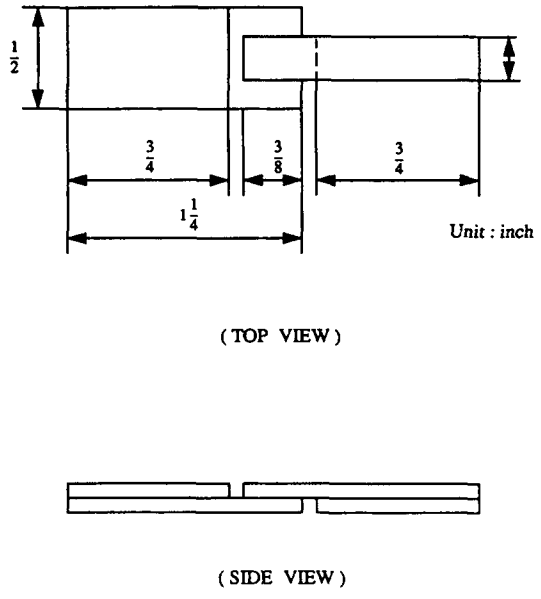


**Figure 2** Form and dimensions of the modified single lap-shear joint specimen.

men as depicted in Figure 2.[15] Gloves were worn to prevent the specimen surface from becoming contaminated. The sized PEEK films were wiped with methanol and put into a mechanically pumped vacuum chamber for 1 day to be dried completely. After drying, the single lap-shear joint specimens were placed between two thin plates of Pyrex glass for handling, then put in the mold which was already heated to the expected bonding temperature. Also, to prevent the specimens from adhering to the Pyrex glass, Kapton tape was used between them. The temperature was controlled within a fluctuation of ±2°C during processing. The mold was closed and a small amount of pressure (≈ 17 psi) applied to promote good contact and wetting for the desired time. The entire mold was then cooled to room temperature under pressure.

### Fracture Test

All bonded specimens were shear-tested by loading in tension at room temperature with an Instron testing machine at a crosshead speed of $5.0 \times 10^{-3}$ in. min, yielding a tensile strain rate of $1.3 \times 10^{-2}$/ min over the lapped gauge length. To obtain accurate results, 10 specimens were tested under each set of conditions. Specimen alignment in the grips of the Instron with respect to the tensile axis was very important to minimize the bending moment during testing. The resultant self-bonding strength was expressed as the applied maximum tensile load at the break divided by the contacting bond area.

### Microscopy Observation

Before the shear test, the bonding area of the specimens was observed by using C-mode scanning acoustic microscopy (Sonoscan C-SAM 3100 system) to measure the degree of wetting at each bonding condition. Also, scanning electron microscopy was performed using a Hitachi S-450 scanning election microscope (SEM) to observe the crystalline morphology and distribution in PEEK specimens bonded at different conditions. For this purpose, the specimens were properly etched by a permanganic technique before SEM examination.[16] Figure 3(a) and (b) represent the specific area of the specimen observed by C-SAM and SEM, respectively. After the shear test, the resultant fracture surfaces were examined with the SEM.

## RESULTS AND DISCUSSION

### Self-Bonding Strength Measurement

Comparative self-bonding strengths for different bonding times at each constant bonding temperature are summarized in Table I. The standard deviation

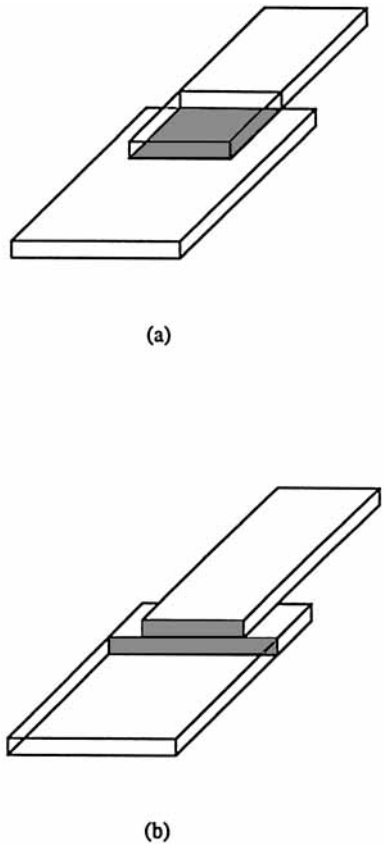


**Figure 3** Specific area of the specimen observed by (a) C-SAM and (b) SEM.

for a set of 10 specimens at each bonding condition was within ±5% of the mean. The resultant values listed in the table for 270 and 300°C show the shear test results measured on specimens having the bonding area reduced to half of the original to prevent tensile failure. Because all specimens bonded at 300°C fractured in tension at an edge of the overlap, the values of self-bonding strength at this condition are actually higher than those listed in Table I. The self-bonding strength increases with time at constant temperature and with temperature at constant time. The self-bonding strength increases faster with increasing time at higher temperatures, especially those in Region III.

Using a polynominal least-squares method,[17] the resultant self-bonding strengths as a function of time at constant temperature in Regions I and II as well as at constant temperature in Region III are plotted in Figure 4(a) and (b), respectively. From Wool's theory, the time dependence of the self-bonding strength is expressed by the equation[14]

$$\sigma = \sigma_0 + Kt^{1/4} \quad (1)$$

where $\sigma$ = self-bonding strength (fracture strength), $\sigma_0$ = developed strength due to wetting, $K$ = constant, and $t$ = bonding time. To investigate the correspondence to the above equation, each self-bonding strength was replotted against the bonding time to the one-fourth power as shown in Figure 5(a) and (b). These figures show that the self-bonding strength varies linearly with $t^{1/4}$ for all bonding conditions.

The above result suggests that the self-bonding strength developed between two surfaces of PEEK film is closely related to diffusion of polymer chains at the interface during the bonding process. In this study, the diffusion effect on the development of the

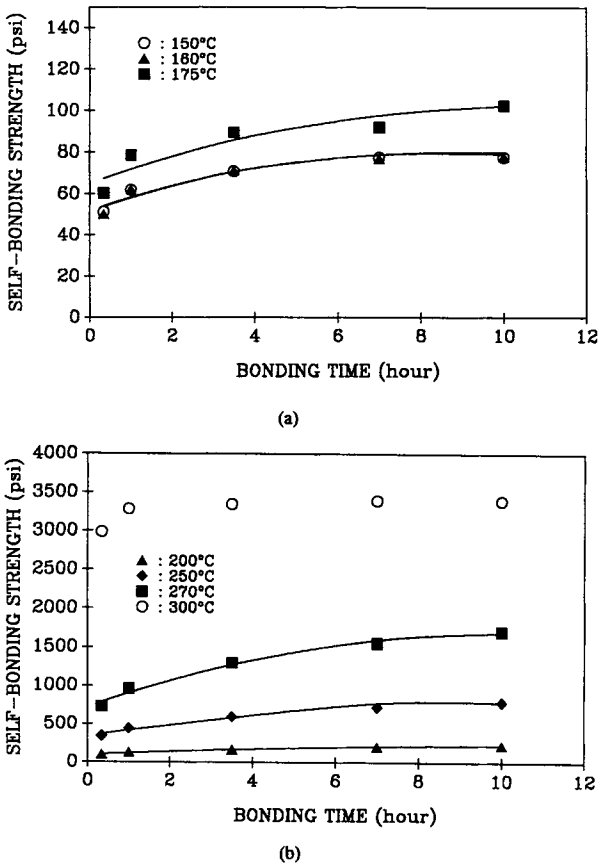


**Figure 4** Plots of self-bonding strength vs. time at various bonding temperatures.

self-bonding strength is described by first measuring the slope of each plot in Figure 5(a) and (b). When analyzed with eq. (1), the slope is considered as a constant $K$. Table II lists the slope values at different bonding temperatures determined by a linear regression analysis. Figure 6 shows a plot of the slope as a function of the bonding temperature. According

**Table I Self-bonding Strengths at Various Bonding Conditions (Under a Constant Pressure of 17 psi)**

| | | Time | | | | |
|---|---|---|---|---|---|---|
| Region | Temp (°C) | 20 min | 1 h | 3.5 h | 7 h | 10 h |
| I | 150 | 51.2 | 61.8 | 70.8 | 77.5 | 77.6 |
| | 160 | 50.1 | 62.1 | 71.2 | 76.9 | 78.0 |
| II | 175 | 60.3 | 78.5 | 89.4 | 91.8 | 102.5 |
| III | 200 | 98.3 | 127.4 | 165.0 | 203.8 | 225.8 |
| | 250 | 344.0 | 440.5 | 598.7 | 721.0 | 790.0 |
| | 270 | 730.5[a] | 960.3[a] | 1298.5[a] | 1550.6[a] | 1702.3[a] |
| | 300 | 2988.5[b] | 3280.2[b] | 3344.0[b] | 3392.8[b] | 3384.3[b] |

[a] The bonding area of the specimen was half of the original.
[b] The bonding area of the specimen was half of the original and tensile fracture occurred at the edge of the overlap.

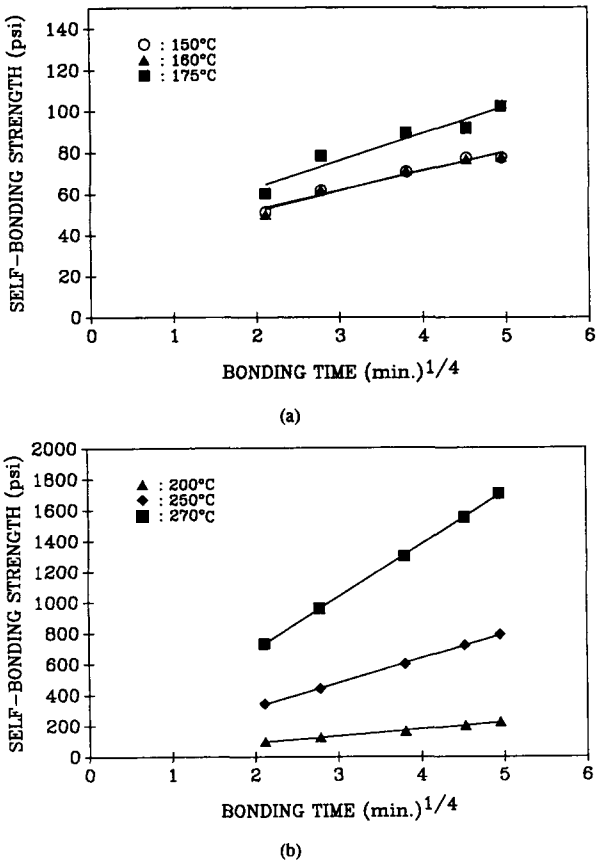


**Figure 5** Plots of self-bonding strength vs. (time)$^{1/4}$ at various bonding temperatures.

to this plot, the slope in Regions I and II increases slowly with the temperature followed by a sharp increase in Region III. Clearly, the interdiffusion of polymer chains during bonding is strongly dependent on the bonding temperature as well as on the bonding time. But the sharp increase of slope $K$ in Region III can not be explained by only the diffusion effect of polymer chains during the bonding process. For this reason, an equation describing the relationship between the slope $K$ and the temperature is needed.

Generally, an increase in temperature accelerates the motion of the polymer chains, bringing the system more rapidly to equilibrium. The temperature dependence of the diffusivity can be expressed by the following equation[18,19]:

$$D_T = A_0 T e^{-Q/RT} \tag{2}$$

where $D_T$ = diffusivity at a temperature $T$, $A_0$ = constant, $T$ = absolute temperature, $Q$ = activation energy, and $R$ = gas constant. From Wool's theory,[15] the constant $K$ in the eq. (1) is defined as

**Table II Changes with Temperature in the Slope $K$ of Eq. (1)**

| Region | Temperature (°C) | Slope ($K$) |
|---|---|---|
| I | 150 | 9.35 |
| | 160 | 9.62 |
| II | 175 | 13.10 |
| III | 200 | 44.26 |
| | 250 | 157.51 |
| | 270 | 340.41 |

$$K = C_0(D_T)^{1/4} \tag{3}$$

where $C_0$ = constant. From Eqs. (2) and (3), the relationship between slope $K$ and temperature $T$ can be expressed by the following equation:

$$K = Z_0 T^{1/4} e^{-Q/4RT} \tag{4}$$

where $Z_0$ = constant. Equation (4) can be converted into the following equation by taking the logarithm of both sides:

$$\text{Ln}(K) - 1/4\ \text{Ln}(T) = -Q/4R(1/T) + \text{Ln}(Z_0) \tag{5}$$

Figure 7 shows a plot of [Ln($K$) − 1/4 Ln($T$)] vs. $1/T$. From eq. (5), if the self-bonding strength is controlled by only diffusion effects as a function of temperature, the plot shown in Figure 7 should have a constant slope of $-Q/4R$, but the resultant slope changes with temperature. In general, thermoplastic polymers have an activation energy of around 20 kcal/mole for diffusion.[13] If the activation energy for diffusion in PEEK is 20 kcal/mol and if the self-bonding strength can be developed by only diffusion of polymer chains during bonding, a dotted line in Figure 7 shows the ideal

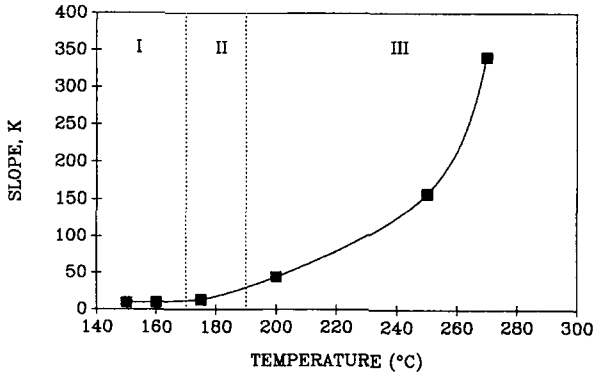


**Figure 6** Effect of temperature on the slope $K$ of eq. (1).

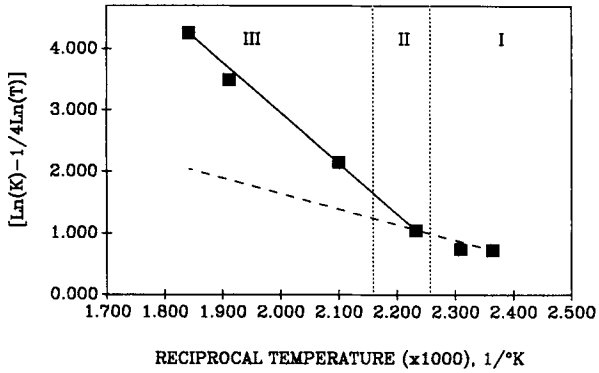


**Figure 7** Plot of [Ln($K$) − 1/4 Ln($T$)] vs. reciprocal temperature ($1/T$).

**Table III Crystallinity Changes with Time and Temperature**

| Region | Temp (°C) | Time 20 min | 1 h | 3.5 h | 7 h | 10 h |
|---|---|---|---|---|---|---|
| I | 150 | 6.99 | 6.81 | 7.73 | 10.30 | 15.40 |
| | 160 | 19.69 | 22.85 | 23.55 | 23.76 | 24.19 |
| II | 175 | 24.39 | 24.71 | 25.42 | 25.40 | 25.27 |
| III | 200 | 24.34 | 25.48 | 25.94 | 26.06 | 27.17 |
| | 250 | 26.17 | 26.70 | 26.81 | 27.91 | 28.85 |
| | 300 | 26.74 | 30.07 | 32.48 | 33.57 | 34.83 |

relationship between [Ln($K$) − 1/4 Ln($T$)] and $1/T$. However, the actual values of [Ln($K$) − 1/4 Ln($T$)] at higher temperatures (represented as a solid line) show a big deviation from the dotted line and the calculated activation energy from the solid line is around 66 kcal/mol. This deviation increases much more with increasing temperature, especially in Region III. Usually, in order for nucleated crystals to grow across the interface of PEEK films after diffusion of the polymer chains during bonding, they must overcome a critical free-energy barrier consisting of both fusion and diffusion terms. At temperatures well below the melting point, the diffusion activation free-energy term is large and indeed is probably the controlling factor. Physically, the polymer chain must diffuse through other disordered chains across the interface and then it must diffuse to the growing crystal nucleus. Therefore, the difference between the two plots in Figure 7 can be explained by considering this additional diffusion activation energy term for crystalline growth.

## Crystallinity Measurement

To measure the degree of crystallinity of the specimen, differential scanning calorimetry (DSC) was performed using a Perkin-Elmer DSC-4 with a thermal analysis data station (TADS) system. The change in the degree of crystallinity with holding time at each bonding temperature is summarized in Table III and plotted in Figure 8. At temperatures of 150 and 160°C in Region I, the change in the degree of crystallinity with time is very small at short times and then increases slowly with increasing time. At a temperature of 175°C in Region II, the degree of crystallinity attains a maximum value of about 25% within very short time and there is no change thereafter. This result supports the conclusion that most of the crystallinity is produced by cold crystallization and the additional crystallization due to annealing effects is negligible. At temperatures of 200, 250, and 300°C in Region III, PEEK specimens crystallize to a degree roughly the same as the maximum value attained in Region II within a very short time. Some slight additional crystallization occurs at each temperature as time increases. This additional crystallization is caused by the annealing effect at each temperature. Thus, the degree of crystallinity in Region III is controlled by both the cold crystallization and the crystallization due to annealing.

## Observation of Crystallinity Change During Cooling

In this research, the bonding process for developing the self-bonding strength at the interface of two PEEK films consists of two stages: The first stage is very fast heating of the PEEK specimens up to the expected bonding temperature and maintaining (annealing) it for a desired bonding time under a

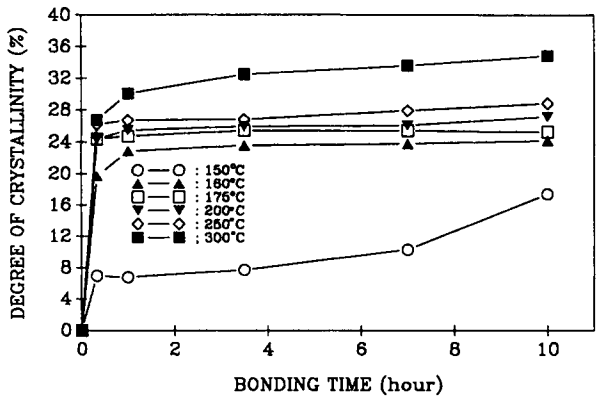


**Figure 8** Effect of bonding time on degree of crystallinity at various bonding temperatures.

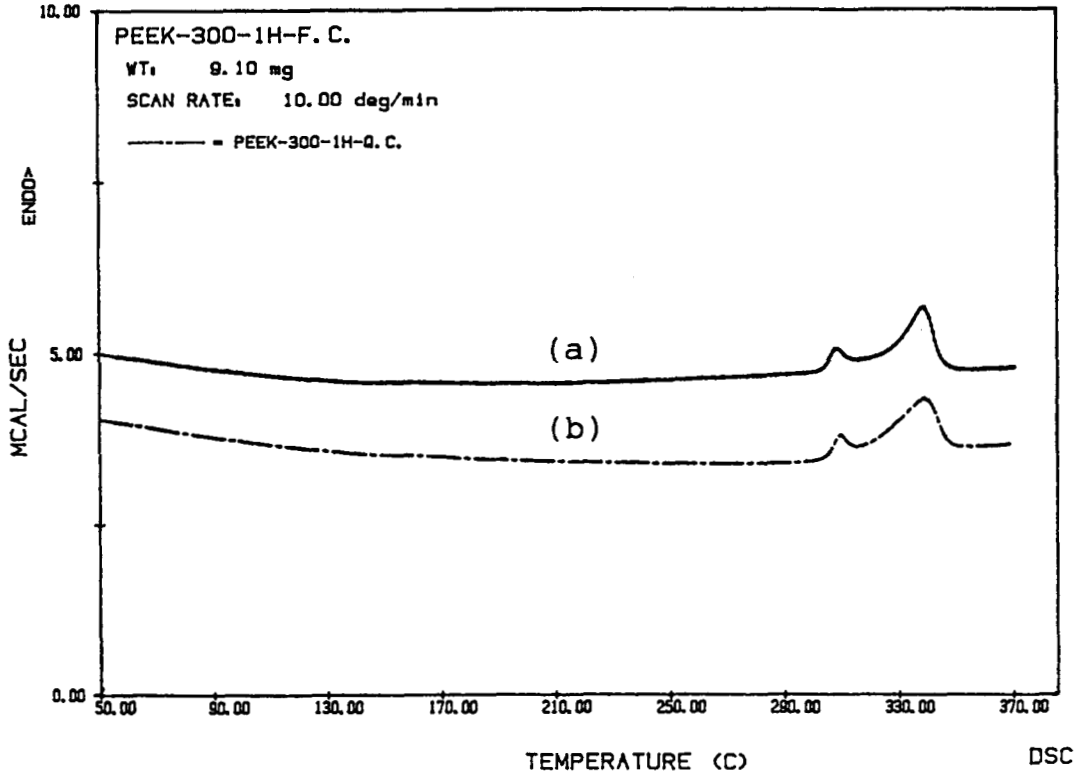


**Figure 9** Typical DSC scans of PEEK samples: (a) is for slowly cooled and (b) is for quenched.

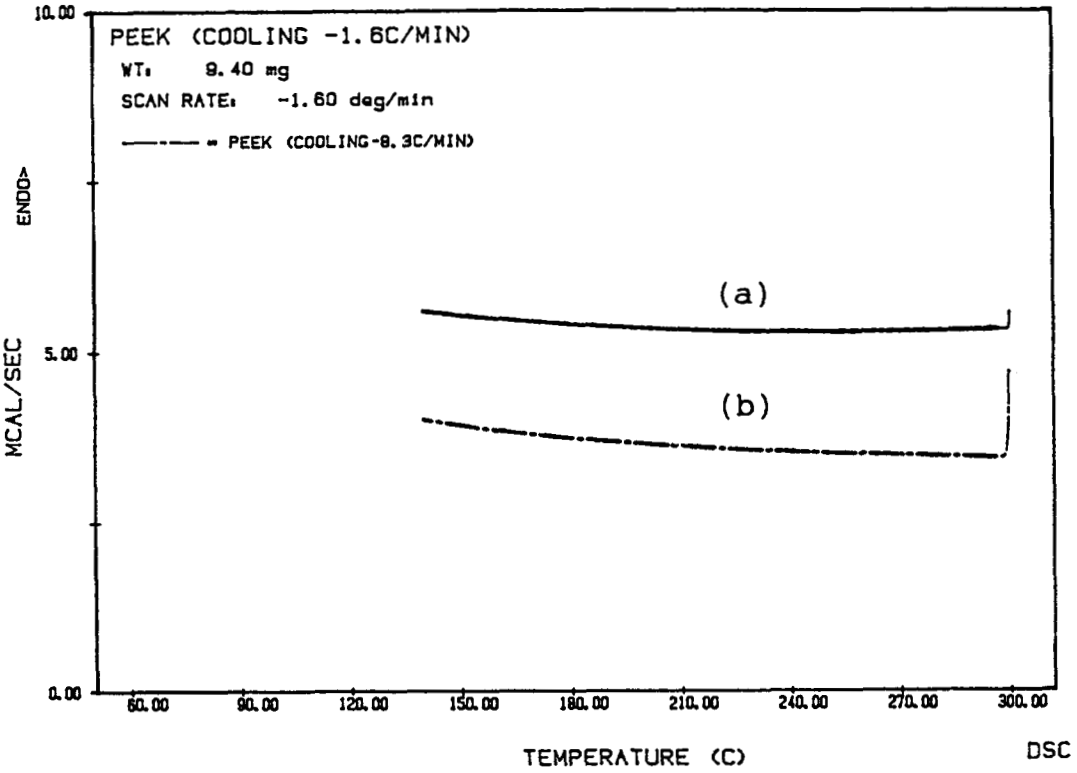


**Figure 10** Typical DSC cooling scans of PEEK samples cooled from 300°C at a cooling rate of (a) −1.6°C/min and (b) −8.3°C/min.

**Table IV Effect of Time on the Degree of Wetting at Different Temperatures (Under a Constant Pressure of 17 psi)**

| | Time (h) | | |
|---|---|---|---|
| Temperature (°C) | 1 | 3.5 | 10 |
| 150 | 97.26 | 97.95 | 99.48 |
| 160 | 98.43 | 98.45 | 98.75 |
| 175 | 97.70 | 98.14 | 98.26 |
| 200 | 98.67 | 98.65 | 98.80 |
| 250 | 97.01 | 97.96 | 98.47 |
| 300 | 97.79 | 97.64 | 98.81 |

constant pressure; the second stage is slowly cooling it down to room temperature. Therefore, to discuss the influence of crystallization on developing the self-bonding of PEEK, it is critical to examine whether or not the slow cooling process affects the crystallization behavior of PEEK.

For this purpose, two pieces of PEEK film were heat-treated in the mold for a time duration equivalent to each bonding condition. After the desired time, one was quenched in ice water to prevent further crystallization and the other was slowly cooled to room temperature in the mold at exactly the same cooling rate as in the cooling stage. Then, the degree of crystallinity of each specimen was measured by DSC. Figure 9 shows the resultant DSC scans of both specimens that were heat-treated at 300°C for 1 h. Scan (a) is for the slowly cooled PEEK specimen and scan (b) is for the quenched one. As shown in this figure, there is no difference between the two DSC scans. Further, the resultant degree of crystallinity calculated from each DSC scan shows the same value of about 30.5%.

To support the above conclusion that no additional crystallization occurs in the cooling stage, another approach was accomplished by using DSC. For this approach, the cooling rate during the cooling process from each bonding temperature to room temperature was measured. When the PEEK specimen is cooled down in the mold from each bonding temperature, it is cooled down at a higher cooling rate at the beginning. Then, as the cooling proceeds to the lower temperature, the cooling rate becomes gradually slower. In the case of a PEEK specimen bonded at the highest bonding temperature of 300°C in this research, the highest cooling rate and the lowest one during cooling were −8.3 and −1.6°C/min, respectively. To observe a PEEK sample having the same thermal history as that of the bonding process, about 10 mg of amorphous PEEK was prepared and heated up to the bonding temperature at the maximum heating rate of 200°C/min in the DSC. After holding the sample for a desired time, it was cooled down at different cooling rates of −8.3 and −1.6°C/min to observe any crystallization during cooling. The resultant DSC scans at each condition are shown in Figure 10. In this study, each DSC scan was recorded down to the glass transition temperature of PEEK (143°C) as there is no further chain motion in PEEK below this temperature. From this figure, it is apparent that no crystallization occurs during the cooling process. Based on these results, it is clear that all crystallization during the bonding process occurs only in the heating and annealing stage and no additional crystallization occurs in the cooling stage.

## Degree of Wetting

According to Wool's theory of crack healing in polymers, polymer chains activated during the bonding process can diffuse across the interface and form physical crosslinks only in the wetted area.[14] Therefore, the self-bonding strength at each bonding condition primarily depends first on the degree of wetting in the bonding area. The degree of wetting at each bonding condition was measured to establish the relationship between the degree of wetting and the self-bonding strength.

Ideally, when two separate PEEK films contact one another under a bonding condition, wetting should occur concurrently at all locations of the bonding area. To cause complete wetting at the interface, complete mechanical contact between two surfaces of the material must first occur. Practically, due to surface roughness of the material, wetting cannot begin instantaneously at all locations. The comparative degrees of wetting between PEEK films at different bonding conditions were determined us-

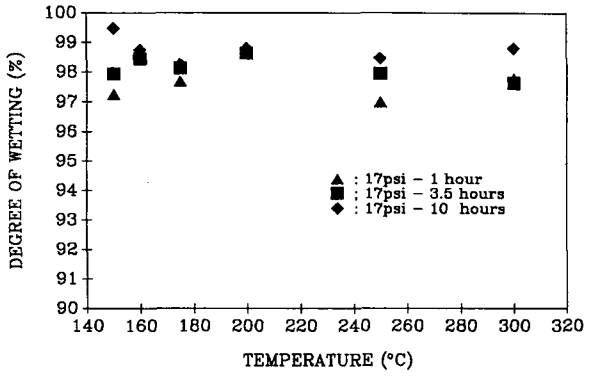


**Figure 11** Effect of temperature on degree of wetting for different times.

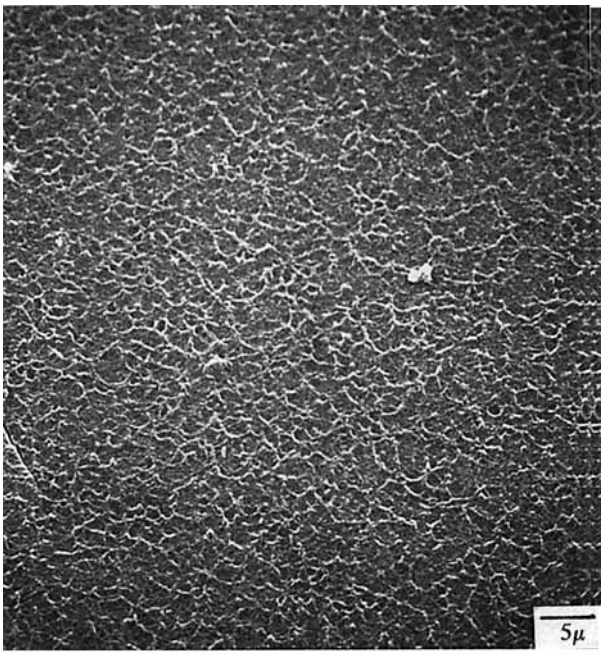


(A) 160°C-1hr-17 psi

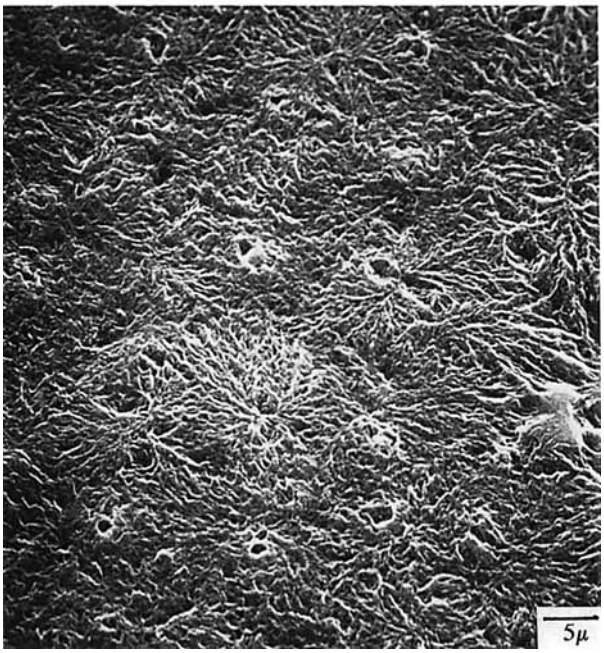


(B) 175°C-10hrs-17 psi

**Figure 12** SEM micrographs of PEEK specimens bonded at different conditions.

ing C-SAM and are summarized in Table IV. The degree of wetting is over 97% for all bonding conditions.

Figure 11 shows the degree of wetting as a function of temperature for different bonding times at a bonding pressure of 17 psi. The effect of temperature at the beginning stage of wetting cannot be deduced from this figure because the wetting process apparently was accomplished in most of the bonding area within a time less than 1 h at all bonding temperatures. In this figure, the degree of wetting varies randomly in the range of 97–100% regardless of the bonding temperature. Clearly, the wetting process in the time range of 1–10 h is independent of temperature and requires very little contact pressure.

This result is at first not consistent with the result that the self-bonding strength increases dramatically as the bonding temperature increases. To explain the inconsistency between the degree of wetting and the self-bonding strength as a function of temper-

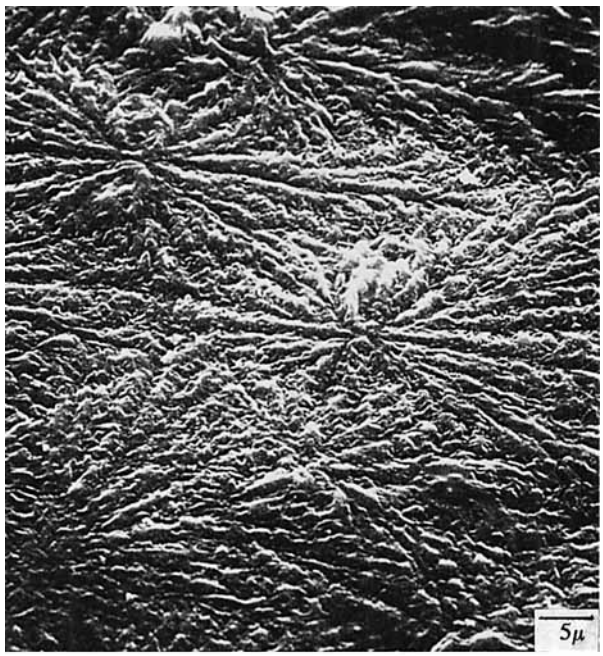


(C) 270°C-1hr-17 psi

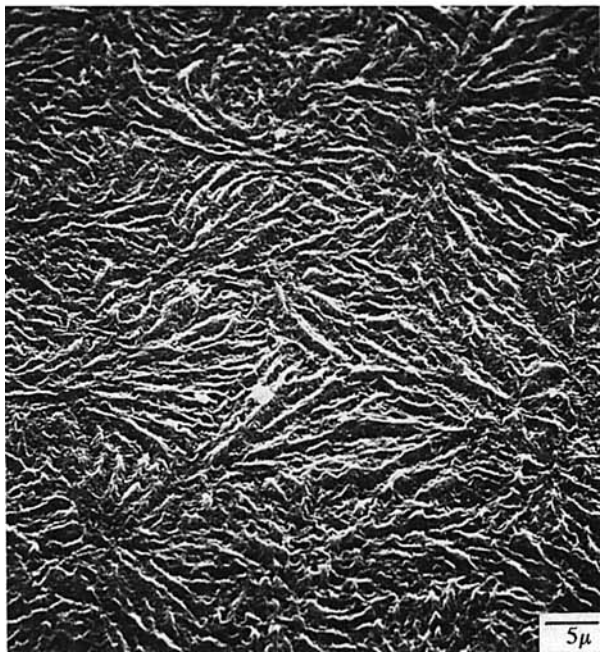


(D) 270°C-10hrs-17 psi

**Figure 12** (*Continued from the previous page*)

ature, there must be a big difference in the diffusion rate of polymer chains in the wetted area as the temperature changes. Thus, even though the degree of wetting shows a nearly identical high value at all bonding temperatures, higher self-bonding strengths at higher bonding temperatures can still be obtained due to higher diffusion rates. Therefore, it is clear that wetting is a necessary but not sufficient condition for self-bonding of PEEK films.

## Crystalline Morphology of PEEK

The internal morphology of PEEK was investigated by SEM observation following a proper permanganic etching. Typical SEM micrographs of PEEK specimens bonded at different conditions are shown in Figure 12(A)–(D). Figure 12(A) shows an SEM micrograph of a specimen bonded at 160°C for 1 h. In this micrograph, what may be a very fine and highly dis-

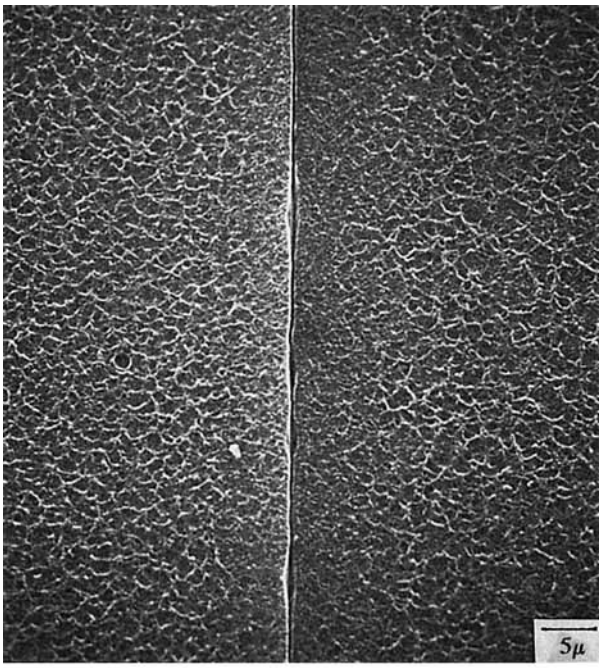


(A) 160°C-1hr-17 psi

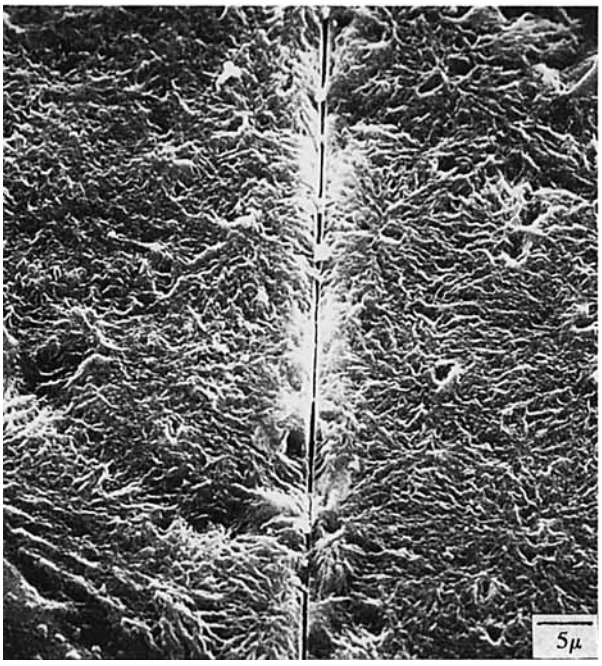


(B) 175°C-10hrs-17 psi

**Figure 13** Microstructures around the interface of PEEK specimens bonded at different conditions.

organized crystalline structure is exhibited, but there is no recognizable spherulitic growth pattern. In the case of a specimen bonded at a slightly higher temperature of 175°C for a longer time of 10 h, better-developed spherulites are observed as shown in Figure 12(B). As the bonding temperature increases, the spherulites become larger in size. Figure 12(C) and (D) show SEM micrographs of specimens bonded at the highest bonding temperature of 270°C for 1 and 10 h, respectively. As the bonding temperature increases, much bigger and better-organized spherulitic patterns are definitely found in the whole area.

Based on the above crystalline morphology observation, the final spherulitic size depends on temperature and time.[20] The general trend of increasing spherulitic size with increasing bonding temperature

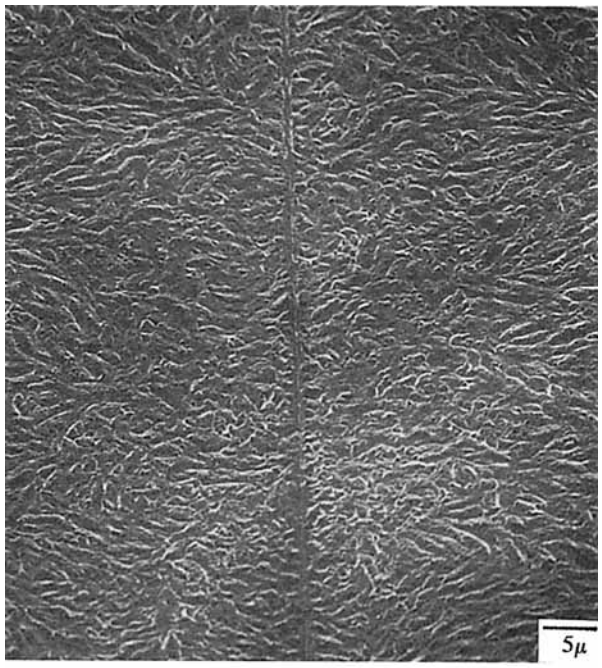


(C) 250°C-1hr-17 psi

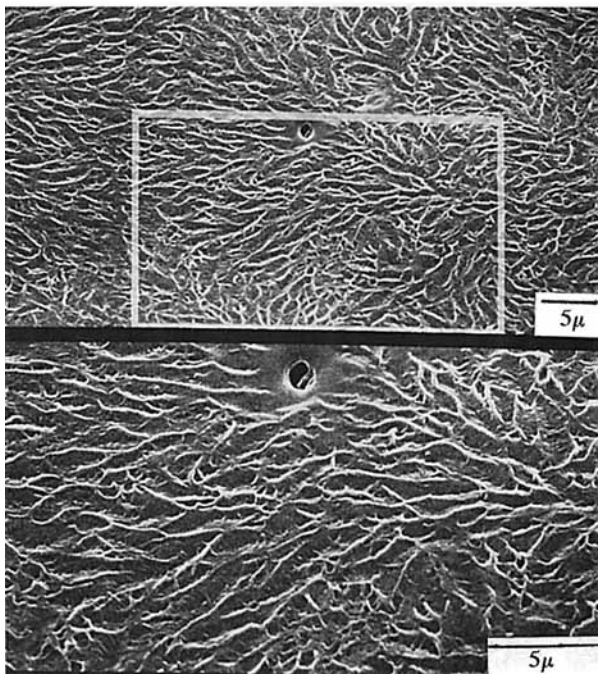


(D) 250°C-10hrs-17 psi

**Figure 13** (*Continued from the previous page*)

can be explained by different nucleation densities at different temperatures. Crystals usually grow outward from the nucleation sites until they meet with their neighbors. Therefore, a higher nucleation density at lower temperatures restricts nucleated crystals from growing larger because they easily impinge on one another. The same is true for bonding time; if the bonding time is long enough, the nucleated crystals can grow larger and form more perfectly.

## Crystalline Growth at the Interface

In considering the self-bonding of amorphous PEEK films, the basic idea is that the physical interface between two PEEK films should disappear during the bonding process to achieve complete bonding. Accordingly, if the interface still exists after the bonding process, this means that the bonding is not complete. A major concern of this study is to clarify

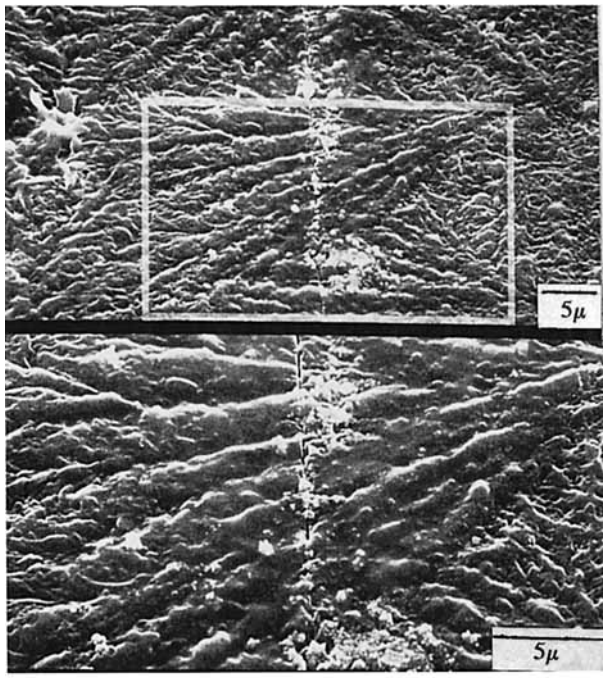


(E) 270°C-1hr-17 psi

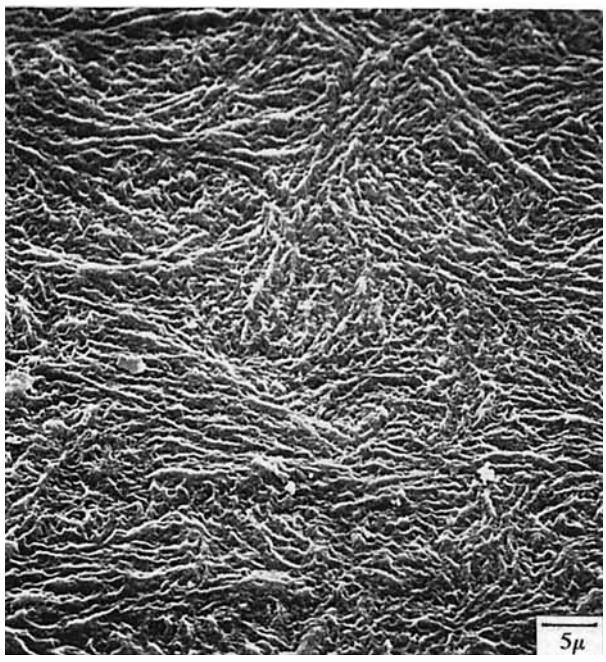


(F) 270°C-10hrs-17 psi

**Figure 13** *(Continued from previous page)*

the role of crystallization in achieving a complete bond at the interface.

Figure 13 shows SEM micrographs of the area around the interface after etching at each bonding condition. By comparing the micrographs in Figure 12 taken in the film bulk not near the surfaces, it is found that the microstructure around the interface exhibits the same features as found farther away from the interface. There does not appear to be a morphology gradient as one moves toward the interface area. Figure 13(A) shows the micrographs of a specimen bonded at 160°C for 1 h. It is clearly observed that although the interface cannot be detected before etching,[15] it clearly reappears after etching. This indicates that the interface was etched more than the other area due to poor bonding at this condition. Figure 13(B), bonded at 175°C for 10 h, also is similar to Figure 13(A). In this figure, although several spheru-

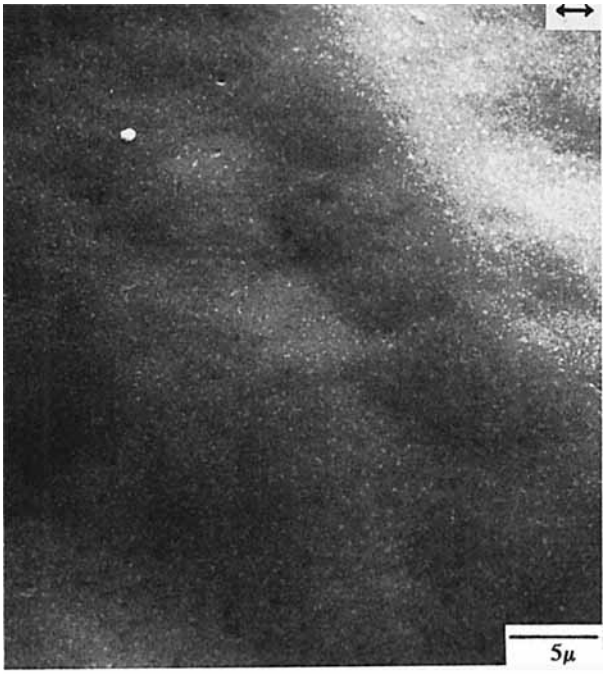


(a) bonded for 1 hour
($\sigma_f$ = 62.1 psi)

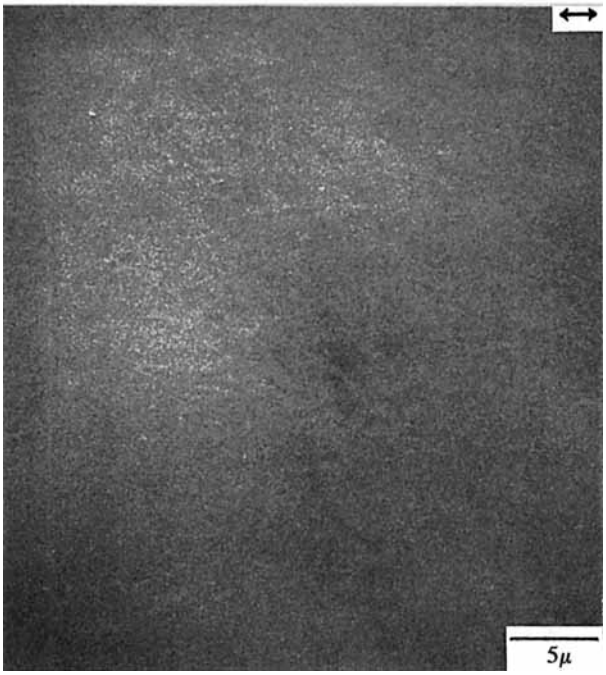


(b) bonded for 10 hours
($\sigma_f$ = 78.0 psi)

**Figure 14** (A) SEM micrographs of the fracture surfaces bonded at 160°C, 17 psi. (B) SEM micrographs of the fracture surfaces bonded at 175°C, 17 psi. (C) SEM micrographs of the fracture surfaces bonded at 200°C, 17 psi. (D) SEM micrographs of the fracture surfaces bonded at 250°C, 17 psi. (E) SEM micrographs of the fracture surfaces bonded at 270°C, 17 psi.

lites have developed on each side of the interface, there is no evidence of crystalline growth across the interface. In the cases of specimens bonded at higher temperatures in Region III, however, the resultant micrographs are different from those of specimens bonded at lower temperatures. Figure 13(C) shows micrographs of a specimen bonded at 250°C for 1 h. In this figure, the interface can still be observed after etching, but its trace is very vague and unclear. Micrographs of a specimen bonded at the same temperature of

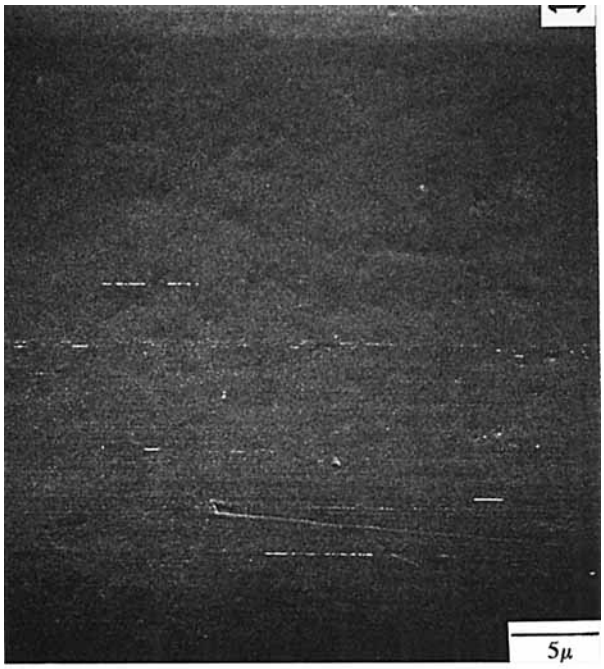


(a) bonded for 1 hour
($\sigma_f$ = 78.5 psi)

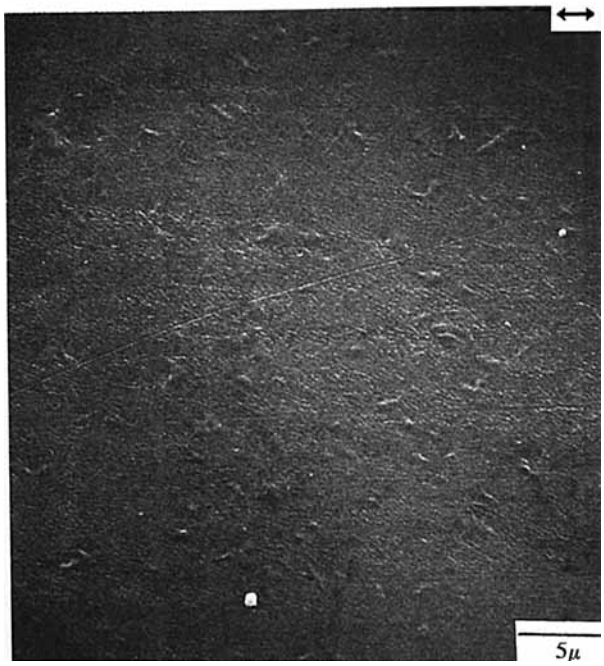


(b) bonded for 10 hours
($\sigma_f$ = 102.5 psi)

**Figure 14** *(Continued from the previous page)*

250°C but for a longer bonding time of 10 h are shown in Figure 13(D). In this figure, the lower part of the SEM micrograph is magnified from the white rectangle area in the upper part. A small hole positioned in the center is believed to be the mark of the interface caused by a dirt imperfection at that spot. In this micrograph, it is clearly observed that numerous spherulite arms grew across the interface and tightly intertwined with themselves. At the same time, the interface completely disappeared. In general, for the crystalline phase to grow across the interface, diffusion of the polymer chains across the interface must occur first. It is clear that the rate of diffusion and resultant entanglement of the polymer chains across the interface is much faster at a higher bonding temperature. Figure 13(E) shows micrographs of a specimen bonded at 270°C

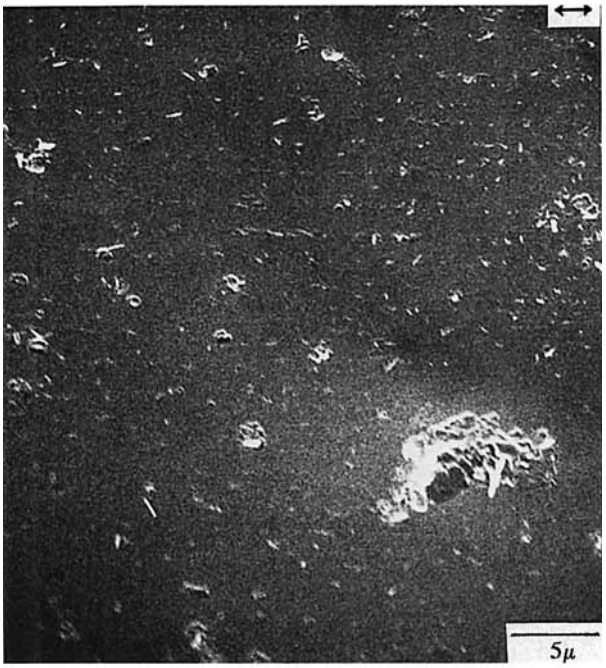


(a) bonded for 1 hour
($\sigma_f$ = 127.4 psi)

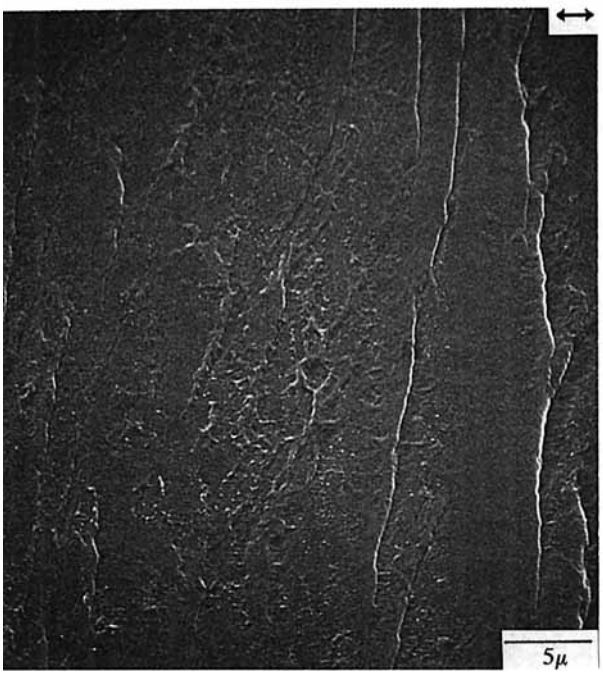


(b) bonded for 10 hours
($\sigma_f$ = 225.8 psi)

**Figure 14** *(Continued from the previous page)*

for 1 h. As shown in this micrograph, many spherulites were developed around the interface and grew across the interface. An additional interesting feature of the micrograph is that some of the disconnected interface still remains between the spherulite arms. Figure 13(F) shows micrographs of a specimen bonded at 270°C for 10 h. As expected, no interface is observed and the microstructure around the interface cannot be distinguished from that farther away from the interface.

The crystalline morphology observation near the interface strongly shows that self-bonding of PEEK is achieved by crystalline growth following diffusion and entanglements of the polymer chains across the interface.

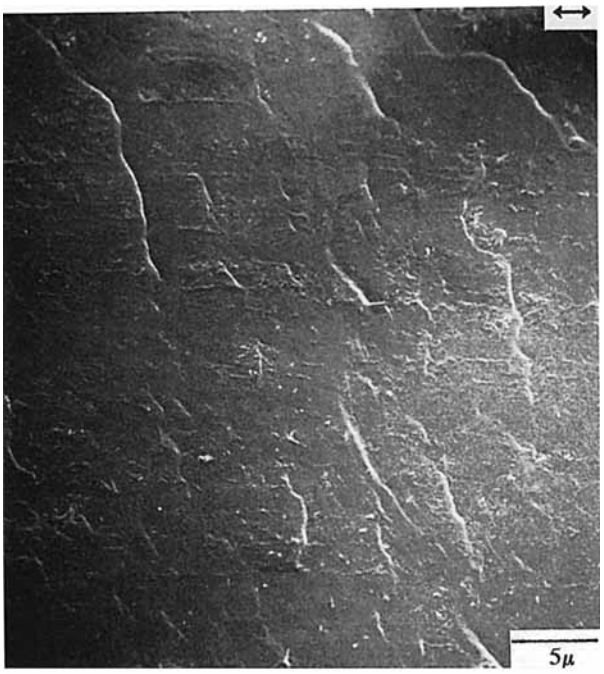


(a) bonded for 1 hour
($\sigma_f$ = 440.5 psi)

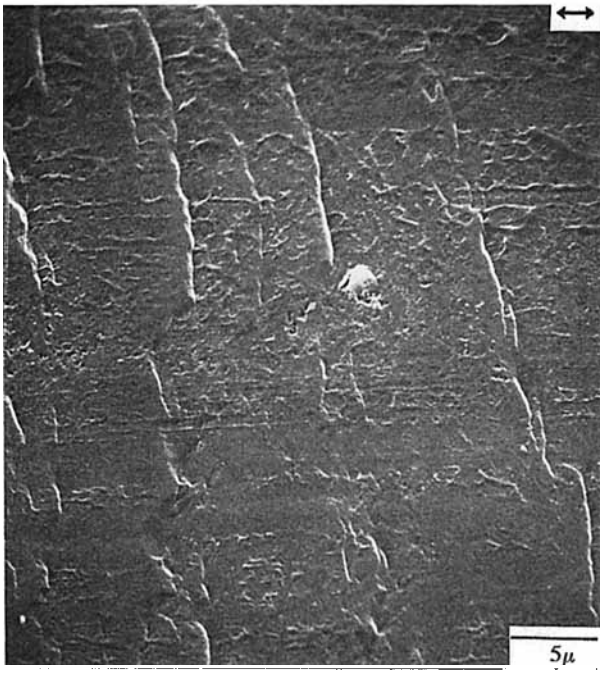


(b) bonded for 10 hours
($\sigma_f$ = 790.0 psi)

**Figure 14** *(Continued from the previous page)*

## Fracture Surface Characterization

Single lap-shear joint specimens bonded at different conditions were shear-tested and the resultant fracture surfaces were observed under the SEM. Figure 14(A)–(F) shows the resultant fracture surfaces at various bonding conditions. The arrow indicates the direction of the applied load during the shear test.

The SEM micrographs of (a) and (b) in Figure 14(A) show the fracture surfaces bonded at 160°C for different bonding times of 1 and 10 h, respectively. Both micrographs exhibit a very smooth and plain fracture surface regardless of the bonding time. It is clear that very poor interaction of the polymer chains occurred between the two PEEK surfaces during this bonding process. As a result, the speci-

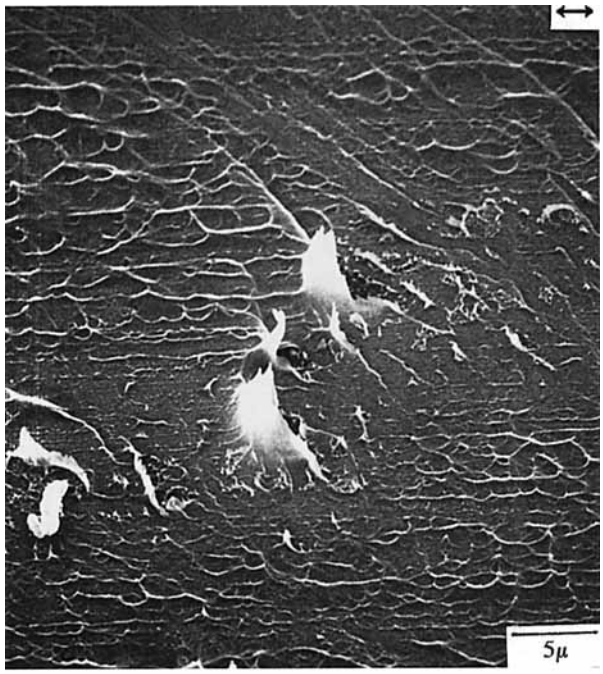


(a) bonded for 1 hour
($\sigma_f$ = 960.3 psi)

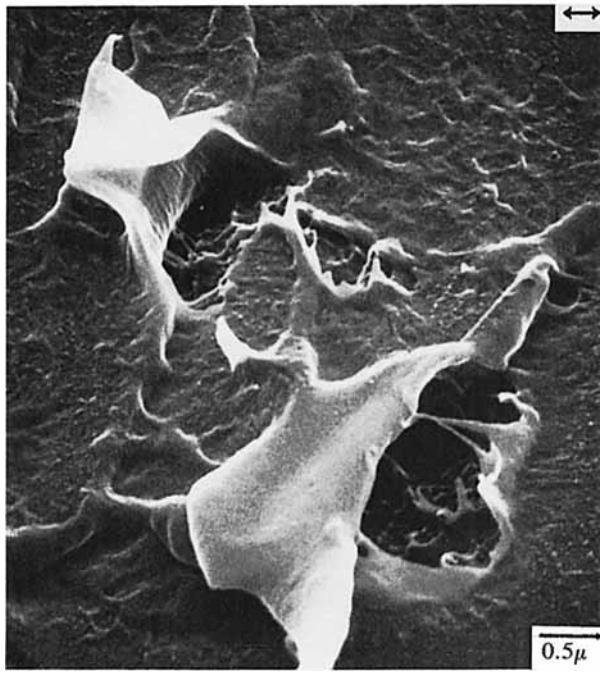


(b) bonded for 1 hour
($\sigma_f$ = 960.3 psi)

**Figure 14** *(Continued from the previous page)*

mens bonded at this condition also showed very poor self-bonding strength. Similar fracture surfaces were observed in the specimens bonded at 175°C as shown in Figure 14(B). In this figure, many tiny popped-out spots were observed in micrograph (b) bonded for a longer bonding time of 10 h. Otherwise, the fracture surface shows the same features as shown in the previous condition. But, as the bonding temperature increases further, the resultant fracture surface shows more complicated features. Figure 14(C) shows SEM micrographs of the fracture surface bonded at 200°C. In a specimen bonded for 1 h at this temperature, a pockmarked surface was observed as shown in micrograph (a). Some spots were much bigger and deeper than were others. This result is believed to be caused by locally different

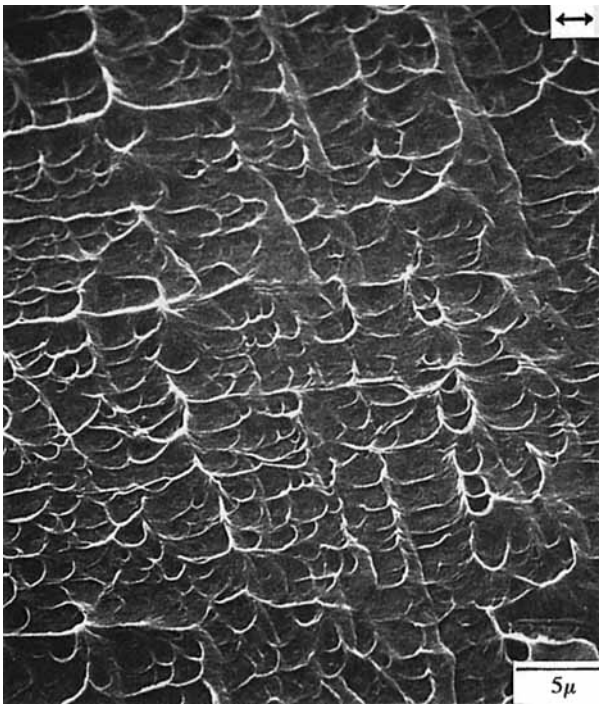


(c) bonded for 10 hours ($\sigma_f$ = 1702.3 psi)

**Figure 14** *(Continued from the previous page)*

bonding strength and subsequent yielding during fracture. In the specimen bonded for 10 h, some striation patterns perpendicular to the direction of the applied load were exhibited [micrograph (b)]. In the case of bonding at 250°C, much denser striation patterns were clearly observed over the whole area as shown in Figure 14(D). An additional feature in the fracture surface, dimplelike patterns with the striations, begins to be observed in micrograph (b) of the sample bonded for 10 h. Figure 14(E) shows SEM micrographs of the fracture surface bonded for 1 h at 270°C. In micrograph (a), much clearer dimplelike patterns with striations are observed. Micrograph (b) shows large flaps of pulled-out polymer typical of microcracking and ductile crack propagation. Furthermore, in the case of the specimen bonded for 10 h, completely clear dimplelike ductile fracture patterns are uniformly distributed over the whole area as shown in micrograph (c).

The fracture surfaces clearly depend on the bonding condition. Comparing the fracture surfaces with the self-bonding strengths at different bonding conditions shows that the fracture surface features change in the sequential order of smooth surface, popped-out surface, striations, and dimplelike patterns as the self-bonding strength increases. As discussed before, more crystals were growing across the interface in the specimen bonded at a higher bonding temperature. Accordingly, when a crack begins to propagate, those crystals growing across the interface create a barrier to the crack propagation. As the applied load increases, the crack overcomes the resistance of the crystalline barrier and propagates in a ductile manner through them. In this case, the resistance of the crystalline barrier to crack propagation definitely affects the self-bonding strength at the interface. Therefore, when the crack propagates in the specimen having a higher self-bonding strength, better-developed ductile fracture features such as striations, and dimplelike patterns are created in the resultant fracture surface.

## CONCLUSIONS

The self-bonding mechanism of amorphous PEEK film can be explained by crystalline growth after diffusion and entanglement of the polymer chains across the interface as a function of time and temperature. For the polymer chains to diffuse across the interface, wetting between two separate PEEK films must first occur. Only a small amount of pressure (< 17 psi) is needed to enhance good wetting at the contacted area.[15] The experimental results show that wetting is not a sufficient condition for the development of the self-bonding strength of PEEK films. When two pieces of PEEK film are bonded at a higher temperature, the activated polymer chains can diffuse much faster and entangle themselves across the interface than can occur at a lower temperature. As a result, more crystals can grow across the interface and the interface begins to disappear, leading to a much higher self-bonding strength at a higher bonding temperature and a longer bonding time.

The experimental results imply that the self-bonding of amorphous PEEK films offers a great potential for developing excellent bond strength approaching the strength of the parent material without any adhesives. For example, in autoclave processing cycles, the key to excellent mechanical performance is bonding at a proper temperature for a proper time. Experimentally, the processing window for self-bonding of PEEK is a temperature region above the cold crystallization (185°C) and before melting (335°C). Roughly, a few hours at 300°C are sufficient to generate a well-bonded PEEK laminate which will not suffer delamination at extremely low compression loads, as has been a problem in some high $T_g$ thermoplastic composite systems.

The partial financial support of this work by McDonnell Douglas Corp. under Contract No. WS-MDRL-3595 is gratefully acknowledged.

## REFERENCES


1. J. C. Seferis, *Polym. Compos.*, **7,** 158 (1986).
2. D. J. Blundell, J. M. Chalmers, M. W. Mackenzie, and W. F. Gaskin, *SAMPE Q.*, **16,** 22 (1985).
3. J. Kenny, A. D. D'Amore, and L. Nicolais, *SAMPE J.*, **25,** 27 (1989).
4. D. C. Jones, D. C. Leach, and D. R. Moore, *Polymer,* **26,** 1385 (1985).
5. C. Carfagna, E. Amendola, A. D'Amore, and L. Nicolais, *Polym. Eng. Sci.*, **28,** 1203 (1988).
6. D. J. Kemmish and J. N. Hay, *Polymer,* **26,** 905 (1985).
7. D. B. Kline and R. P. Wool, *Polym. Eng. Sci.*, **28,** 52 (1988).
8. R. G. Stacer and H. L. Schreuder-Stacer, *Int. J. Fract.*, **39,** 201 (1989).
9. P. G. de Gennes, *J. Chem. Phys.*, **55,** 572 (1971).
10. Y. H. Kim and R. P. Wool, *Macromolecules,* **16,** 1115 (1983).
11. S. Prager and M. Tirrell, *J. Chem. Phys.*, **75**(10), 5194 (1981).
12. K. Jud, H. H. Kausch, and J. G. Williams, *J. Mater. Sci.*, **16,** 204 (1981).
13. H. H. Kausch, *Polymer Fracture,* 2nd ed., Springer-Verlag, New York, 1987.
14. R. P. Wool and K. M. O'Connor, *J. Polym. Sci. Polym. Lett. Ed.*, **20,** 7 (1982).
15. B.-R. Cho, PhD Thesis, Washington University, 1994.
16. R. H. Olley and D. C. Bassett, *Polymer,* **23,** 1707 (1982).
17. H. S. Mickley, T. K. Sherwood, and C. E. Reed, *Applied Mathematics in Chemical Engineering,* 2nd ed., McGraw-Hill, New York, 1957.
18. W. L. McCabe, J. C. Smith, and P. Harriott, *Unit Operations of Chemical Engineering,* 5th ed., McGraw-Hill, New York, 1993.
19. J. M. McKelvey, *Polymer Processing,* Wiley, New York, 1962.
20. S. Kumar, D. P. Anderson, and W. W. Adams, *Polymer,* **27,** 329 (1986).


*Received September 30, 1994*
*Accepted December 1, 1994*